



Published in final edited form as:

Circulation. 2012 October 23; 126(17): 2051–2064. doi:10.1161/CIRCULATIONAHA.112.121830.

Transient Receptor Potential Canonical-3 Channel–Dependent Fibroblast Regulation in Atrial Fibrillation

Masahide Harada, MD, PhD,

Department of Medicine and Research Center, Montreal Heart Institute and Université de Montréal, Montreal, Quebec, Canada

Xiaobin Luo, MSc,

Department of Medicine and Research Center, Montreal Heart Institute and Université de Montréal, Montreal, Quebec, Canada

Xiao Yan Qi, PhD,

Department of Medicine and Research Center, Montreal Heart Institute and Université de Montréal, Montreal, Quebec, Canada

Artavazd Tadevosyan, MSc,

Department of Medicine and Research Center, Montreal Heart Institute and Université de Montréal, Montreal, Quebec, Canada

Ange Maguy, PhD,

Department of Medicine and Research Center, Montreal Heart Institute and Université de Montréal, Montreal, Quebec, Canada

Balazs Ordog, PhD,

Department of Medicine and Research Center, Montreal Heart Institute and Université de Montréal, Montreal, Quebec, Canada

Jonathan Ledoux, PhD,

Department of Medicine and Research Center, Montreal Heart Institute and Université de Montréal, Montreal, Quebec, Canada

Takeshi Kato, MD, PhD,

Department of Medicine and Research Center, Montreal Heart Institute and Université de Montréal, Montreal, Quebec, Canada

Patrice Naud, PhD,

Department of Medicine and Research Center, Montreal Heart Institute and Université de Montréal, Montreal, Quebec, Canada

Niels Voigt, MD,

Division of Experimental Cardiology, Medical Faculty Mannheim, University of Heidelberg, Mannheim, Germany

Yanfen Shi, PhD,

Copyright © 2012 American Heart Association, Inc. All rights reserved.

Correspondence to Stanley Nattel, 5000 Belanger St E, Montreal, Quebec, H1T 1C8, Canada. stanley.nattel@icm-mhi.org.

Disclosures

Dr Van Wagoner is the recipient of a research grant from Gilead Pharma to evaluate the impact of an A2b antagonist on AF inducibility/fibrosis in a canine model. Dr Nattel is listed as an inventor on a patent requested by his employer (TRPC3 channels in AF). The other authors report no conflicts.

The online-only Data Supplement is available with this article at <http://circ.ahajournals.org/lookup/suppl/doi:10.1161/CIRCULATIONAHA.112.121830/-/DC1>.

Department of Medicine and Research Center, Montreal Heart Institute and Université de Montréal, Montreal, Quebec, Canada

Kaichiro Kamiya, MD, PhD,

Department of Cardiovascular Research, Research Institute of Environmental Medicine, Nagoya University, Nagoya, Japan

Toyoaki Murohara, MD, PhD,

Department of Cardiology, Nagoya University Graduate School of Medicine, Nagoya, Japan

Itsuo Kodama, MD, PhD,

Department of Cardiovascular Research, Research Institute of Environmental Medicine, Nagoya University, Nagoya, Japan

Jean-Claude Tardif, MD,

Department of Medicine and Research Center, Montreal Heart Institute and Université de Montréal, Montreal, Quebec, Canada

Ulrich Schotten, MD, PhD,

Department of Physiology, Maastricht University, Maastricht, Netherlands

David R. Van Wagoner, PhD,

Department of Molecular Cardiology, Cleveland Clinic, Cleveland, OH

Dobromir Dobrev, MD, and

Division of Experimental Cardiology, Medical Faculty Mannheim, University of Heidelberg, Mannheim, Germany

Stanley Nattel, MD

Department of Medicine and Research Center, Montreal Heart Institute and Université de Montréal, Montreal, Quebec, Canada

Abstract

Background—Fibroblast proliferation and differentiation are central in atrial fibrillation (AF)—promoting remodeling. Here, we investigated fibroblast regulation by Ca^{2+} -permeable transient receptor potential canonical-3 (TRPC3) channels.

Methods and Results—Freshly isolated rat cardiac fibroblasts abundantly expressed TRPC3 and had appreciable nonselective cation currents (I_{NSC}) sensitive to a selective TRPC3 channel blocker, pyrazole-3 (3 $\mu\text{mol/L}$). Pyrazole-3 suppressed angiotensin II-induced Ca^{2+} influx, proliferation, and α -smooth muscle actin protein expression in fibroblasts. Ca^{2+} removal and TRPC3 blockade suppressed extracellular signal-regulated kinase phosphorylation, and extracellular signal-regulated kinase phosphorylation inhibition reduced fibroblast proliferation. TRPC3 expression was upregulated in atria from AF patients, goats with electrically maintained AF, and dogs with tachypacing-induced heart failure. TRPC3 knockdown (based on short hairpin RNA [shRNA]) decreased canine atrial fibroblast proliferation. In left atrial fibroblasts freshly isolated from dogs kept in AF for 1 week by atrial tachypacing, TRPC3 protein expression, currents, extracellular signal-regulated kinase phosphorylation, and extracellular matrix gene expression were all significantly increased. In cultured left atrial fibroblasts from AF dogs, proliferation rates, α -smooth muscle actin expression, and extracellular signal-regulated kinase phosphorylation were increased and were suppressed by pyrazole-3. MicroRNA-26 was downregulated in canine AF atria; experimental microRNA-26 knockdown reproduced AF-induced TRPC3 upregulation and fibroblast activation. MicroRNA-26 has NFAT (nuclear factor of activated T cells) binding sites in the 5' promoter region. NFAT activation increased in AF fibroblasts, and NFAT negatively regulated microRNA-26 transcription. In vivo pyrazole-3

administration suppressed AF while decreasing fibroblast proliferation and extracellular matrix gene expression.

Conclusions—TRPC3 channels regulate cardiac fibroblast proliferation and differentiation, likely by controlling the Ca²⁺ influx that activates extracellular signal-regulated kinase signaling. AF increases TRPC3 channel expression by causing NFAT-mediated downregulation of microRNA-26 and causes TRPC3-dependent enhancement of fibroblast proliferation and differentiation. In vivo, TRPC3 blockade prevents AF substrate development in a dog model of electrically maintained AF. TRPC3 likely plays an important role in AF by promoting fibroblast pathophysiology and is a novel potential therapeutic target.

Keywords

arrhythmia; calcium; ion channels; fibrillation; remodeling

Atrial fibrillation (AF) is the most common arrhythmia in clinical practice, and it confers significant morbidity and mortality.^{1,2} Because the utility of conventional antiarrhythmic agents that target cardiac ion channels is limited by inefficacy and side effects, new treatment strategies are required.¹⁻³ An improved understanding of underlying mechanisms may help in the design of novel therapies.² Under pathological conditions, cardiac fibroblasts first proliferate and then differentiate into myofibroblasts that secrete profibrotic extracellular matrix (ECM).^{3,4} Atrial fibrotic remodeling causes conduction abnormalities and may promote fibroblast-cardiomyocyte electric interactions that favor AF occurrence and maintenance.^{5,6} Therefore, fibroblast control mechanisms could constitute novel antiarrhythmic targets. Although it is known that cellular Ca²⁺ homeostasis regulates fibroblast function,⁶ the precise regulatory mechanisms remain unclear.

Transient receptor potential (TRP) channels, activated by cell stretch and other pathological stimuli, regulate cellular Ca²⁺ entry.⁶ TRP channels modulate fundamental cell functions such as cell proliferation and death.⁶⁻⁸ Mechanical stretch and related stimuli contribute to arrhythmic substrates³; TRP channels are candidates to link arrhythmic remodeling stimuli to arrhythmia-promoting cardiac fibroblast responses. In preliminary studies (online-only Data Supplement Figure I), we noted cell-selective expression of TRP canonical-3 (TRPC3) subunits in freshly isolated fibroblasts, along with TRPC3 downregulation on fibroblast differentiation to myofibroblasts, which identified TRPC3 as a potential modulator of fibroblast function. We undertook the present study to test the following hypotheses: (1) TRPC3 subunits play a role in fibroblast function in normal hearts and in an AF model; (2) fibroblast TRPC3 expression is upregulated in AF under the control of discrete microRNA-related molecular mechanisms; and (3) in vivo TRPC3 inhibition can suppress AF-associated remodeling.

Methods

A detailed description of methods used in this study is available in the online-only Data Supplement.

Cardiac Fibroblast Isolation and Culture

Fibroblasts were isolated from adult rat or dog hearts as described previously.⁹ Tissues were digested with collagenase II and cardiomyocytes removed by low-speed centrifugation and passage through a 20- μ m nylon filter. Fibroblasts were concentrated by high-speed centrifugation (2000 rpm, 10 minutes). Freshly isolated fibroblasts or cells in primary culture within 3 days of isolation (online-only Data Supplement Figure II-A) were used in most experiments. Long-term cultured first-passage cells (2–3 weeks), which express α -

smooth muscle actin (α -SMA) and show actin fiber organization (online-only Data Supplement Figure II-B), were used in rat myofibroblast studies.

Atrial Tissue Samples From Humans, Goats, and Dogs

Right atrial (RA) appendage biopsy samples were obtained from patients in sinus rhythm and with chronic AF during coronary artery bypass graft surgery after informed consent as approved by the ethics review committee of Dresden University of Technology. AF was induced in chronically instrumented goats by use of repetitive burst pacing for 10 days.¹⁰ Dogs with congestive heart failure (CHF) with an AF substrate were created by ventricular tachypacing (240 bpm, 2 weeks).¹¹ Normal goats and dogs were used as controls. RA tissue samples were collected and fast-frozen in liquid N₂.

AF Dogs

A total of 48 mongrel dogs (weight, 20–36 kg) were divided into control and atrial tachypacing groups. Animal care procedures followed National Institutes of Health guidelines and were approved by the Animal Research Ethics Committee of the Montreal Heart Institute. Dogs were anesthetized with ketamine (5.3 mg/kg IV)/ diazepam (0.25 mg/kg IV)/isoflurane (1.5%), intubated, and ventilated. A unipolar pacing lead was inserted into the RA appendage under fluoroscopic guidance and connected to a pacemaker in the neck. Bipolar electrodes were inserted into the right ventricular apex and RA appendage for electrogram recording. Atrioventricular block/ventricular pacing (used in many studies of atrial tachycardia remodeling¹²) was not performed, to more closely mimic spontaneous clinical AF episodes. The atrial pacemaker was programmed to stimulate the RA at 600 bpm for 1 week, with fibrillatory atrial activity maintained during pacing as assessed by daily ECG and intracardiac recordings. Echocardiography was performed on day 0 (baseline) and day 7 to assess left atrial (LA) dimension, LA systolic function, and left ventricular diastolic volume.

For in vivo pyrazole-3 (Pyr3) treatment of AF dogs, ALZET osmotic pumps were implanted subcutaneously in the back to continuously administer intravenous Pyr3 (0.1 mg · kg⁻¹ · d⁻¹ in DMSO and polyethylene glycol) or vehicle during atrial tachypacing (online-only Data Supplement Figure III).

Electrophysiological Studies

A terminal open chest electrophysiological study was performed on day 7. Dogs were anesthetized with morphine (2 mg/kg SC) and α -chloralose (120 mg/kg IV, followed by 29.25 mg · kg⁻¹ · h⁻¹) and ventilated. After performance of a median sternotomy, the atrial effective refractory period and mean AF duration induced by burst pacing were measured as described previously.¹²

TaqMan Low-Density Arrays

RNA was extracted with TRIzol. RNA integrity was assessed via an Agilent bioanalyzer (Agilent Technologies; RNA integrity number >7.5 required). cDNA was synthesized with a high-capacity cDNA reverse transcription kit and random hexamer primers. TaqMan low-density arrays were used in 2-step reverse transcription-polymerase chain reaction (PCR).¹³ Real-time PCR was performed on the 7900HT Fast Real-Time PCR System (Applied Biosystems). TRP subunit genes were investigated by use of inventoried TaqMan assays. The mean expression of genes with a cycle threshold value (Ct) <30 was used as the reference.¹⁴

Whole-Cell Patch Clamping

Whole-cell voltage clamping was performed to record the nonselective cation current (I_{NSC}) at 37°C. The pipette solution contained (in mmol/L) 135 CsCl, 0.1 CaCl₂, 10 EGTA, 4.0 MgATP, 1.0 MgCl₂, 10 HEPES, 6.6 sodium phosphocreatine, 0.3 Na-GTP (pH 7.4/CsOH). The bath solution contained (in mmol/L) 140 NaCl, 5.4 TEA-Cl, 2.0 CaCl₂, 1.0 MgCl₂, 10 HEPES, 10.0 glucose (pH 7.4/CsOH). Nifedipine (5 μmol/L) was used to block any L-type Ca²⁺ current. Na⁺ current was inactivated with a holding potential of 0 mV. Currents were elicited with 3-second voltage-ramp protocols (0.07 mV/ms, from -110 mV to 100 mV, 0.1 Hz) at a holding potential of 0 mV.¹⁵

Cell Proliferation and Cell-Cycle Analysis

Cardiac fibroblasts were cultured in T25 culture flasks (2.0×10⁵ cells/flask, 25 cm² growth area) for each treatment group. After incubation, cells were harvested after trypsinization and then fixed with ice-cold 75% ethanol. Samples were stored at -20°C until analysis. Pelleted cells were resuspended and incubated (4°C, 30 minutes) in staining solution that contained propidium iodide. Cell numbers and DNA content frequency histograms were obtained via FACScan (constant flow rate, 60 μL/min; 5-minute acquisition time).

Western Blots

Protein was extracted, quantified, and processed.^{12,16} Cytoplasmic and nuclear protein fractions were extracted from fresh fibroblasts with a ProteoExtract subcellular proteome extraction kit (Calbiochem). Protein samples were separated by gel electrophoresis and transferred to polyvinylidene difluoride membranes. Membranes were blocked and incubated with mouse anti- α -SMA, anti-phospho-p44/42-MAP kinase, anti-TRPM7, anti-NFATc3, anti-HSP70, anti-lamin A/C and anti-vimentin, rabbit anti-TRPC3, anti-TRPC1, anti-calsequestrin, and anti-NFATc4 antibodies. Secondary antibodies conjugated to horseradish peroxidase were used for detection via chemiluminescence.

Confocal Imaging

Cultured, freshly isolated fibroblasts or LA tissue cryosections were fixed with 2% paraformaldehyde, washed with PBS, and incubated with mouse anti- α -SMA, goat anti-vimentin, mouse anti-NFATc3, and rabbit anti-NFATc4, followed by donkey anti-mouse IgG Alexa Fluor 555, donkey anti-rabbit IgG Alexa Fluor 488, donkey anti-goat IgG Alexa Fluor 488, and/or TOPRO 3 iodide. Apoptosis was assessed by TUNEL (terminal dUTP nick end-labeling) assay with ApopTag. Fluorescent images were obtained via a Zeiss LSM-710 or Olympus FluoView FV1000 inverted confocal microscope.

Ca²⁺ Imaging

Primary cultured rat fibroblasts (1-day culture) were loaded with Fluo-4 (10 μmol/L) in phenol-free M199 medium in the presence of pluronic acid (2.5 μg/mL) for 50 minutes. Ca²⁺ imaging was obtained with an Andor Revolution confocal system and a iXon (Andor Technologies) mounted on an upright Nikon FN-1 microscope. Fluo-4 was excited at 488 nm; emitted fluorescence was collected at 495 nm. Images (512×512 pixels) were acquired at 15 frames/second. F₀ was determined by averaging fluorescence from 10 consecutive baseline images.¹⁷

Quantitative PCR

To study microRNA, RNA/microRNA were extracted with a TRIzol/ mirVana miRNA extraction kit (Ambion). Real-time reverse transcription-PCR was performed with 6-carboxy fluorescein-labeled fluorogenic TaqMan primers. Fluorescence signals were detected in

duplicate, normalized to $\beta 2$ -microglobulin RNA for total RNA and to U6 small nuclear RNA for microRNA, and quantified with MxPro qPCR software (Stratagene).¹⁶

TRPC3 Knockdown

TRPC3 knockdown lentivirus vector plasmid was obtained from Open Biosystems (Oligo ID: V2LMM_11490). A scrambled micro-RNA-adapted shRNA (shRNAmir)-overexpressing virus was used as a negative control. For lentivirus infection, 3-day cultured fibroblasts were plated in T25 culture flasks at 4×10^3 cells/cm², infected at 50 MOI, and incubated for 3 days before experiments were performed.

MicroRNA (miR) Overexpression/Knockdown

For overexpression, sense and antisense oligoribonucleotides were synthesized by Invitrogen, and the double-stranded RNA was created by an annealing treatment. A scrambled RNA was the negative control. For knockdown, antisense anti-miR oligonucleotides (AMO26a) with locked nucleic acid technology were synthesized by Exiqon. Scrambled oligonucleotides with methylene bridges were used as negative controls. Dog LA fibroblasts in primary culture were transfected with miR-26a duplex (100 nmol/L), AMO26a (10 nmol/L), and/or control sequences with Lipofectamine 2000 (Invitrogen).¹⁸

Dual Luciferase Reporter Assay

A fragment that contained the miR target sequence was synthesized by Invitrogen and used as a template for PCR amplification. The PCR product was subcloned in the pMIR-REPORT luciferase miR expression reporter vector. HEK293 cells were transfected with 50 ng of pMIR-REPORT, 0.5 ng of pRL-TK (for internal control), and miR-26a duplex (10 nmol/L) and/or AMO26a (3 nmol/L) with Lipofectamine 2000.

Statistical Analysis

Data are presented as mean \pm SEM. A 2-way ANOVA with multiple-group comparisons (Bonferroni-corrected *t* test) was applied to data with 2 main effect factors. One-way ANOVA was applied for single main effect factor experiments. Repeated-measure analyses were used when the same sets of subjects or materials were exposed to multiple interventions. Student *t* tests were used for comparisons that involved only 2 groups. For multiple comparisons with Bonferroni correction, adjusted probability values were calculated by multiplying original probability values by the number of comparisons (*N*) performed; values shown are adjusted values (*N* \times *P*). Two-tailed *P*<0.05 was considered statistically significant. For additional details, see the online-only Data Supplement.

Results

TRPC3-Mediated I_{NSC} and Ca^{2+} Entry

I_{NSC} recordings from freshly isolated rat fibroblasts are shown in Figure 1A and online-only Data Supplement Figure II-C. I_{NSC} was substantially suppressed by superfusion with the TRPC3-selective blocker Pyr3 (Figure 1B)¹⁹ and by the general TRP channel blocker, gadolinium (Gd^{3+} ; 100 μ mol/L; online-only Data Supplement Figure II-C). Passage-cultured myofibroblasts (online-only Data Supplement Figure II-B) showed larger membrane capacitance than fibroblasts (16.8 ± 1.4 versus 6.4 ± 0.4 picofarads, *P*<0.01) but had much smaller Gd^{3+} - and Pyr3-sensitive I_{NSC} , consistent with quantitative PCR data (online-only Data Supplement Figure II-D through II-F).

We then tested whether TRPC3 channels contribute to Ca^{2+} entry in cardiac fibroblasts. Because diacylglycerol has been suggested to be a physiological activator of TRPC3,²⁰ we

examined the effect of TRPC3 blockade on Ca^{2+} entry induced by 1-oleoyl-2-acetyl-*sn*-glycerol (OAG) and angiotensin II, which activate diacylglycerol receptors directly and indirectly, respectively. Both angiotensin II (Figure 1C and 1D) and OAG (online-only Data Supplement Figure IV-A and IV-B) induced fibroblast Ca^{2+} entry, which was prevented by Pyr3, which suggests that TRPC3 channels are needed for OAG- and angiotensin II-induced Ca^{2+} entry.

Role in Fibroblast Proliferation and Differentiation

We next examined whether TRPC3 channel block affects cardiac fibroblast proliferation. Rat cardiac fibroblasts were maintained in the presence or absence of Gd^{3+} , Pyr3, or control vehicle for up to 1 day in primary culture. After 24-hour culture in vehicle medium, the number of fibroblasts increased substantially (Figure 1E). After 1- and 24-hour treatment, fibroblasts were collected for proliferation analysis by flow cytometry. Representative DNA content histograms showing the G_2/M phase cell content, an index of DNA duplication, are provided in online-only Data Supplement Figure V-A and V-B. Pyr3 significantly slowed the increase in fibroblast number and reduced G_2/M phase cell content (Figure 1E and 1F), as did Gd^{3+} (online-only Data Supplement Figure V-C and V-D). Pyr3 also significantly increased the percentage of TUNEL-positive fibroblasts versus control (online-only Data Supplement Figure VI). These data suggest that TRPC3 channels regulate cardiac fibroblast survival and proliferation.

After fibroblasts proliferate, they differentiate into ECM-secreting myofibroblasts characterized by altered morphology and increased α -SMA expression. Online-only Data Supplement Figure VII-A shows confocal images of rat fibroblasts, cultured with or without Pyr3, stained with anti- α -SMA antibodies. The spindle-shaped expansion and α -SMA-enhanced expression associated with myofibroblast differentiation were inhibited by 3- $\mu\text{mol/L}$ Pyr3. Figure 1G shows representative α -SMA immunoblots on cultured rat fibroblasts; α -SMA protein expression was decreased significantly by Pyr3 (Figure 1H). Thus, TRPC3 channels participate in fibroblast differentiation into myofibroblasts. We also examined the effect of TRPC3 blockade on already differentiated myofibroblasts. Consistent with downregulation of TRPC3 in myofibroblasts, their cell number, G_2/M phase cell content, and α -SMA expression were unchanged by Pyr3 (online-only Data Supplement Figure VII-B through VII-D). Thus, once fibroblasts differentiate into myofibroblasts, TRPC3 channels no longer appear to be involved in their regulation.

TRPC3-Mediated Ca^{2+} Entry, ERK-1/2 Phosphorylation, and Fibroblast Activation

We then examined whether TRPC3-mediated Ca^{2+} entry acts by modulating Ca^{2+} -dependent extracellular signal-regulated kinase (ERK)-1/2 activation, which affects cell survival and fibroblast activation.^{21,22} Fibroblasts were cultured for 24 hours in 3 conditioned media: (1) 0.4 mmol/L Ca^{2+} , (2) 2.4 mmol/L Ca^{2+} , and (3) 2.4 mmol/L Ca^{2+} with Pyr3. ERK-1/2 phosphorylation was decreased significantly in low- $[\text{Ca}^{2+}]$ medium and with exposure to Pyr3 (Figure 2A). Next, we examined the effect of extracellular Ca^{2+} concentration on fibroblast proliferation. The increase in cell number of cultured fibroblasts and the G_2/M phase cell content were significantly smaller with less $[\text{Ca}^{2+}]$ in the culture medium (Figure 2B and 2C). A selective ERK pathway inhibitor, PD98058 (50 $\mu\text{mol/L}$), also significantly reduced the number of fibroblasts and the G_2/M phase cell content after 24-hour culture (Figure 2D and 2E). The data in Figure 2 suggest that TRPC3-mediated Ca^{2+} influx contributes to the ERK-1/2 activation that regulates fibroblast proliferation.

TRPC3 Knockdown Suppresses Atrial Fibroblast Proliferation

We were unable to study TRPC3 knockdown in rat fibroblasts because spontaneous TRPC3 downregulation in culture was almost complete over the time period needed for lentivirus-

mediated knockdown. However, we noted that TRPC3 downregulation was slower in cultured dog atrial fibroblasts, which were used to study the effects of TRPC knockdown. TRPC3 subunit mRNA and protein expression decreased significantly in TRPC3 shRNA-infected fibroblasts; TRPC6 mRNA remained unchanged (online-only Data Supplement Figure VIII-A and VIII-B). The fold increase in cultured fibroblast cell number was significantly attenuated in TRPC3 shRNA-infected fibroblasts (online-only Data Supplement Figure VIII-C), as was the G₂/M phase cell content (online-only Data Supplement Figure VIII-D), which indicates that TRPC3 channels are involved in canine atrial fibroblast proliferation.

Atrial TRPC3 Expression in Large Animal/Human AF Substrates

To assess a potential role in the AF substrate, we examined the protein expression of TRPC1, TRPC3, and TRPM7 subunits in RA tissue samples from AF patients, AF goats, and CHF dogs with an AF substrate. Atrial TRPC3 expression increased significantly in all groups with AF substrates (online-only Data Supplement Figure IX-A through IX-C), whereas TRPC1 and TRPM7 remained unchanged (online-only Data Supplement Figure IX-D through IX-I).

Atrial Remodeling in Dogs With Electrically Maintained AF

To examine further the potential role of TRPC3 in AF, we used a canine model of electrically maintained AF. Representative surface and intracardiac day 7 ECG recordings showing irregular, rapid atrial activity and irregular ventricular responses typical of AF are shown in Figure 3A. Spontaneous AF was maintained after pacing cessation. Fibrillatory electric activity and spontaneous postpacing AF were observed consistently during the 1-week pacing period (online-only Data Supplement Figure X). Immediately after tachypacing onset (recordings at 6.0±0.2 minutes after onset), ventricular activation rate increased by 55%, but ventricular rate then returned to control values by day 3 (online-only Data Supplement Figure XI-A). At the end of the study, atrial and ventricular filling pressures were slightly but significantly increased in AF dogs (online-only Data Supplement Table I). Online-only Data Supplement Figure XI-B illustrates atrial structural remodeling in AF dogs, with significant changes in LA diastolic area and fractional area change (online-only Data Supplement Figure XI-C and XI-D).

AF dogs showed electric remodeling manifested by reduced effective refractory periods (Figure 3B) and increased duration of burst-pacing-induced AF (Figure 3C). LA fibrosis and vimentin staining (an index of fibroblast density) were assessed by histomorphometry (Figure 3D). Fibrous tissue content was unchanged (Figure 3E), but vimentin-positive area (Figure 3F) and protein expression (immunoblots, Figure 3G) increased significantly in AF dogs.

TRPC3 Regulation of Atrial Fibroblast Activation in AF Dogs

Figure 4A shows I_{NSC} before and after 3 μmol/L Pyr3 in freshly isolated LA fibroblasts. Pyr3-sensitive current increased significantly in LA fibroblasts of AF dogs (Figure 4B), corresponding to increased TRPC3 subunit protein expression in freshly isolated LA fibroblasts (Figure 4C). ERK phosphorylation (Figure 4D) and ECM gene expression (Figure 4E) were also significantly increased in LA fibroblasts of AF dogs.

The cell number increase rate, G₂/M phase cell content, and α-SMA protein expression all increased in LA fibroblasts of AF dogs (Figure 5A through 5C), which indicates increased fibroblast proliferation and differentiation. In vitro treatment of AF fibroblasts with Pyr3 decreased these fibroblast activation indexes significantly (Figure 5D through 5F). ERK activation was increased significantly in AF (Figure 5G). ERK phosphorylation in AF dogs

was reduced significantly after 24-hour treatment with Pyr3 (Figure 5H). These data suggest that TRPC3 channels are an important contributor to fibroblast activation in AF.

MiR-26 Regulation of TRPC3 Channels

MicroRNAs posttranscriptionally regulate protein expression in many pathological conditions.¹ MiR-target prediction (TargetScan) suggested that miR-26 targets the TRPC3 gene (online-only Data Supplement Figure XII-A). Expression of the 2 miR-26 isoforms, miR-26a and miR-26b, which have identical seed sequences, was decreased significantly in freshly isolated LA fibroblasts from AF dogs (Figure 6A). Other miRs involved in cardiac remodeling¹ were studied, and miR-133 was also downregulated; however, miR-26 was particularly strongly expressed in fibroblasts (Figure 6B), whereas miR-133 expression was cardiomyocyte selective (Figure 6C). Neither miR-1 nor miR-133 targets TRPC3.

We then examined posttranscriptional regulation of TRPC3 by miR-26a with dual luciferase reporter assay. Luciferase vectors carrying the miR-26a target gene sequence of TRPC3 were cotransfected along with miR-26a duplex and/or antisense anti-miR-26a oligonucleotides (AMO26a; online-only Data Supplement Figure XII-B) into HEK-293 cells. MiR-26a overexpression significantly decreased luciferase readout, whereas knockdown of endogenous miR-26a by AMO26a significantly increased luciferase fluorescence (Figure 6D), which indicates that miR-26a regulates TRPC3 translation.

Using immunoblotting, we further validated the effect of miR-26a on TRPC3 protein expression in cultured canine LA fibroblasts. MiR-26a overexpression decreased TRPC3 protein expression significantly, whereas miR-26a knockdown to mimic AF-related miR-26 downregulation increased TRPC3 protein (Figure 6E). We then assessed the regulation of fibroblast proliferation by miR-26a. MiR-26a overexpression significantly decreased fibroblast-number (Figure 6F), as well as G₂/M cell percentage (Figure 6G), whereas miR-26a knockdown increased these fibroblast-proliferation indexes. These data indicate that miR-26a controls TRPC3 expression by downregulating TRPC3 protein and produces parallel changes in fibroblast proliferation indexes.

NFATc3 Regulation of miR-26a

We next looked for the potential mechanism of fibroblast miR-26 control in AF. Nuclear translocation of NFAT (the nuclear factor of activated T cells), subsequent to dephosphorylation by Ca²⁺/calmodulin-dependent calcineurin activation, is important in AF-related cardiomyocyte remodeling.¹ The promoter regions of the host genes for miR-26a/b in humans and dogs are predicted to have multiple binding motifs for NFAT (online-only Data Supplement Figure XII-D). We therefore evaluated cellular localization of NFAT in fibroblasts from AF and control dogs. Figure 7A shows representative confocal images of freshly isolated LA fibroblasts stained with vimentin, TOPRO3 (nuclear stain), and NFATc3/c4 antibodies. Nuclear localization of NFATc3 increased significantly in AF (Figure 7B). We also quantified nuclear NFAT localization by immunoblotting on isolated canine fibroblast nuclei. AF significantly reduced the cytosolic and increased the nuclear protein fraction of NFATc3 (Figure 7C). To assess NFAT regulation of miR-26 gene expression, we examined the effect of incubation with a selective membrane-permeable NFATc3/c4 blocker, INCA6 (2.5 μ mol/L), on miR-26 and TRPC3 expression in canine atrial fibroblasts. INCA6 significantly increased miR-26a/b expression (Figure 7D) and decreased TRPC3 protein expression (Figure 7E), consistent with an inhibitory effect of NFAT on miR-26 transcription. These data suggest that AF-induced NFATc3 translocation suppresses miR-26a transcription, thereby reducing miR-26a inhibition of TRPC3 translation and resulting in TRPC3 protein upregulation.

Effects of In Vivo TRPC3 Blockade on the AF Substrate

To more directly assess the role of TRPC3 in the AF-promoting remodeling of the AF dogs in the present study, additional AF dogs were treated with Pyr3 ($0.1 \text{ mg} \cdot \text{kg}^{-1} \cdot \text{d}^{-1}$ by continuous intravenous infusion) or vehicle for the entire period of atrial tachypacing (online-only Data Supplement Figure III). At the terminal electrophysiological study, Pyr3-treated dogs showed significantly reduced AF duration (Figure 8A). They also had slightly but significantly greater effective refractory period values at short cycle lengths (Figure 8B). Consistent with in vivo TRPC3 control of fibroblast function, Pyr3 significantly decreased LA vimentin expression (Figure 8C), as well as fibroblast number on day 3 (Figure 8D) and G₂/M cell content on day 2 (Figure 8E), in LA fibroblasts cultured from AF dogs. Pyr3 also decreased ECM gene expression in LA fibroblasts freshly isolated from AF dogs (Figure 8F).

Discussion

The present study shows that TRPC3 channels control fibroblast function via Ca²⁺-dependent ERK phosphorylation, which results from Ca²⁺ entry through I_{NSC} . In addition, atrial TRPC3 expression is upregulated in AF, and this change induces fibroblast proliferation, differentiation, and activation. TRPC3 upregulation in AF is caused by down-regulation of its regulatory microRNA, miR-26, under the control of NFATc3. Infusion of a highly selective TRPC3 inhibitor, Pyr3, suppresses development of the AF substrate in a canine model.

Comparison With Previous Studies on TRP Channel–Dependent Regulation of Fibroblast Function

TRPC3 is a Ca²⁺-permeable ion channel that shows 75% homology with TRPC6 and 7.²⁰ These channels show substantial Ca²⁺ permeability and mediate receptor-activated extracellular Ca²⁺ entry.^{20,23,24} TRPC3/6/7 channels are directly activated by diacylglycerol liberation into the plasma membrane, triggered by agonist binding to G protein-coupled receptors, such as angiotensin II and endothelin-1 receptors.^{20,23} TRPC channels are widely expressed and are involved in diverse biological functions, such as neuronal cell survival,²⁴ blood vessel constriction,²⁵ immune cell maturation,²⁶ and cardiac hypertrophy.^{27,28} However, the regulatory role of TRPC3 channels in cardiac fibroblast function has not been reported previously.

Rose et al¹⁵ demonstrated that a TRP channel–like I_{NSC} is elicited by C-type natriuretic peptide in freshly isolated rat ventricular fibroblasts. Transcripts encoding TRPC3 subunits were highly expressed in the fresh fibroblasts, and I_{NSC} was activated by phorbol esters; however, the role of I_{NSC} in fibroblast function was not examined.

Nishida et al²⁹ reported that TRPC1, 3, 6, and 7 mRNAs are detected in neonatal rat fibroblasts and that TRPC6 channels contribute to the regulation of endothelin-1–induced myofibroblast formation through JNK and NFAT signaling. However, in contrast to the present observations regarding TRPC3 channels, ERK-1/2 phosphorylation was not affected by endothelin-1–activated TRPC6 currents. Of note, the Nishida study was performed in neonatal cells, and TRP channel-dependent regulation of fibroblast function may change during development from neonatal to adult conditions.

Du et al³⁰ demonstrated that current that corresponds to TRP melastatin–related 7 (TRPM7), a Ca²⁺/Mg²⁺-permeable channel, is strongly expressed in fibroblasts isolated from RA samples of AF patients and likely plays an important role in AF pathophysiology. shRNA-based TRPM7 knockdown decreased TRPM7-mediated Ca²⁺ influx in cultured atrial fibroblasts and suppressed fibroblast differentiation induced by transforming growth factor-

β stimulation. The present results showed substantial TRPC3 subunit expression and associated current, as well as significant physiological function, in fibroblasts that were freshly isolated or kept under conditions that limited differentiation. Furthermore, TRPC3-dependent current and fibroblast regulation were enhanced in AF dog fibroblasts. The expression and function of TRPC3 channels disappeared after differentiation to myofibroblasts under culture conditions. In contrast, mRNA expression of TRPM7 subunits remained high in myofibroblasts, similar to the findings of Du et al,³⁰ who also showed strong mRNA expression of TRPM7 but not TRPC3 subunits in cultured human atrial fibroblasts. Cardiac fibroblast phenotype changes dynamically during proliferation and differentiation. The present findings suggest that TRPC3 controls proliferation and differentiation of fibroblasts but is downregulated in the end-cell myofibroblast. This negative-feedback system may prevent excessive ECM remodeling. In contrast, TRPM7 is likely the dominant TRP channel in differentiated myofibroblasts.

Du et al³⁰ found increased TRPM7 current in fibroblasts isolated from atrial samples of AF patients but did not have sufficient tissue to perform Western blot studies. We found increased protein expression of TRPC3, but not TRPC1 or TRPM7, by immunoblotting of atrial samples in AF patients, AF goats, and CHF dogs. This observation suggests that the increased TRPM7 function noted by Du et al³⁰ in fibroblasts from AF patients may have been caused by increased membrane trafficking of TRPM7 subunits or altered regulation rather than increased channel expression per se.

Potential Mechanisms

Mio et al³¹ established the 3-dimensional structure of TRPC3 channels with cryo-electron microscopy. TRPC3 channels have both a pore-forming transmembrane domain and a large intracellular domain, representing a “nested box” structure. The latter structure may act as a molecular anchor for signaling complexes. TRPC3-mediated Ca^{2+} influx and an increase in local Ca^{2+} concentration may trigger protein-protein interactions that activate downstream signaling pathways that regulate fibroblast function. A recent study using B lymphocytes demonstrated that TRPC3 channels act as a platform for protein kinase C and that the sustained scaffolding of protein kinase C at the plasma membrane is associated with activation of the ERK-1/2 signaling pathway.³²

ERK-1/2 is a protein kinase and intracellular signaling molecule involved in various biological functions, including cell growth and survival.^{21,22} In the present study, selective inhibition of ERK-1/2 signaling attenuated rat fibroblast proliferation, which suggests that ERK-1/2 signaling contributes to fibroblast function. Olson et al³³ demonstrated that angiotensin-induced increases in intracellular Ca^{2+} and protein kinase C activation in adult rat cardiac fibroblasts synergistically contribute to ERK-1/2 activation and fibroblast proliferation. TRPC3 channels may be particularly important in this situation, because angiotensin II increases cellular production of diacylglycerol, which activates TRPC3 channels. The present data showed that TRPC3 blockade suppresses Ca^{2+} entry caused by angiotensin II, a well-known profibrotic agent, in rat cardiac fibroblasts.

Novelty and Potential Significance

This is the first study to show a role of TRPC3 channels in controlling fibroblast function and the first to indicate that AF activates fibroblasts via TRPC3-related mechanisms. Furthermore, we were able to identify the mechanism of TRPC3 upregulation in AF (reduced miR-26 negative control of TRPC3 translation, caused by enhanced NFATc3 nuclear translocation in AF fibroblasts, which caused enhanced inhibitory NFATc3 regulation of miR-26) and found that a TRPC3 inhibitor suppresses AF-promoting remodeling. An emerging body of evidence indicates that TRP channels act as important

mediators for a wide variety of physiological functions and are a potential target for drug discovery. There is a need to develop novel approaches to AF treatment, and therapies that prevent fibroblast activation are of potentially great interest.⁶ The present findings point to TRPC3 as a candidate target for AF prevention.

Although it is well recognized that AF promotes atrial fibrosis, little information is available about how this happens. In the present dog model, AF upregulated TRPC3 and caused fibroblast activation that depended on TRPC3-related Ca^{2+} entry, which activated ERK phosphorylation. Similar TRPC3 upregulation was observed in atrial samples from AF patients, AF goats, and AF-prone CHF dogs. TRPC3 channels acted primarily in nondifferentiated fibroblasts, enhancing their ability to proliferate and differentiate into myofibroblasts. Once myofibroblasts were formed, TRPC3 channels became downregulated. This behavior of TRPC3 channels has not been described previously: TRPC3 channels promote fibrosis by causing fibroblasts to proliferate and activate but are then downregulated in activated myofibroblasts to prevent a positive-feedback process. The effects of in vivo Pyr3 infusion to prevent enhanced proliferation and ECM expression of fibroblasts from AF dogs, along with the associated suppression of AF promotion, are consistent with an important role for TRPC3 in fibroblast-mediated AF-promoting remodeling.

Although NFAT nuclear translocation has been shown to occur in AF cardiomyocytes and to be involved in cardiomyocyte remodeling,^{1,34} the present study constitutes the first demonstration of AF-associated NFAT changes in fibroblasts and their involvement in AF-related fibroblast remodeling.

Potential Limitations

We cannot exclude the possibility that fibroblast properties were affected by cell isolation and culture. Considering that fibroblasts lose their original properties after lengthy culture intervals, we used cells in short-term primary culture (maximum of 3 days after isolation) in most experiments. However, this approach cannot completely reproduce the complex in vivo milieu. Any extrapolation of these results to human disease should be made cautiously.

Our patch-clamp recording conditions differed from those used by Du et al³⁰ in that they used pipette solutions that were virtually Mg^{2+} -free, whereas our pipettes contained Mg^{2+} at concentrations typically used for cardiac cell patch-clamp recording. TRPM7 currents are strongly suppressed by intracellular Mg^{2+} ,^{35,36} which likely explains why most of the gadolinium-sensitive current we observed was also sensitive to Pyr3. Under our conditions, I_{NSC} would not be expected to contain substantial TRPM7 current and was strongly downregulated in myofibroblasts. Thus, TRPM7 channels play a much larger role than other TRP channels, including TRPC3, in the regulation of Ca^{2+} influx in differentiated myofibroblasts.

The AF dogs in the present study showed increased atrial fibroblast density and signs of fibroblast activation, such as enhanced α -SMA expression (Figure 8C) and ECM gene upregulation (Figure 7E); however, we did not see increased fibrous tissue content in AF dogs. We suspect that the lack of fibrosis was related to the relatively short time (7 days) that the dogs were kept in AF, with longer intervals necessary for fibrosis development. When AF is maintained for longer periods (>3 months), clear fibrosis develops, even when excessive ventricular rates and left ventricular dysfunction are prevented.³⁷ Fibroblast proliferation and differentiation can promote AF by a range of mechanisms that do not require enhanced fibrous tissue content, particularly fibroblast-cardiomyocyte electric interactions.³ The small atrial effective refractory period increases we noted in Pyr3-treated AF dogs may reflect enhanced fibroblast effects on the electrophysiology of coupled

cardiomyocytes.³ Alternatively, a direct role in cardiomyocytes cannot be excluded and should be assessed in follow-up work. Our findings raise many interesting additional questions that need to be answered but are outside the scope of the present study.

Supplementary Material

Refer to Web version on PubMed Central for supplementary material.

Acknowledgments

The authors thank Nathalie L'Heureux, Chantal St-Cyr, Claudia Liebetrau, and Louis-Robert Villeneuve for technical help and France Thériault for secretarial assistance.

Sources of Funding

This study was supported by the Canadian Institutes of Health Research (MOP 44365), Quebec Heart and Stroke Foundation, the MITACS Network, Japanese Heart Rhythm Society/Medtronic Fellowship, Japan Heart Foundation/Japanese Society of Electrocardiology Scholarship, German Center for Cardiovascular Research, and Fondation Leducq (ENAFRA Network, 07/CVD/03).

References

1. Wakili R, Voigt N, Kääh S, Dobrev D, Nattel S. Recent advances in the molecular pathophysiology of atrial fibrillation. *J Clin Invest*. 2011; 121:2955–2968. [PubMed: 21804195]
2. Nattel S. From guidelines to bench: implications of unresolved clinical issues in atrial fibrillation for basic investigations of atrial fibrillation mechanisms. *Can J Cardiol*. 2011; 27:19–26. [PubMed: 21329858]
3. Burstein B, Nattel S. Atrial fibrosis: mechanisms and clinical relevance in atrial fibrillation. *J Am Coll Cardiol*. 2008; 51:802–809. [PubMed: 18294563]
4. Souders CA, Bowers SL, Baudino TA. Cardiac fibroblast: the renaissance cell. *Circ Res*. 2009; 105:1164–1176. [PubMed: 19959782]
5. Burstein B, Comotois P, Michael G, Nishida K, Villeneuve L, Yeh YH, Nattel S. Changes in connexin expression and the atrial fibrillation sub-strate in congestive heart failure. *Circ Res*. 2009; 105:1213–1222. [PubMed: 19875729]
6. Yue L, Xie J, Nattel S. Molecular determinants of cardiac fibroblast electrical function and therapeutic implications for atrial fibrillation. *Cardiovasc Res*. 2011; 89:744–753. [PubMed: 20962103]
7. Inoue R, Jensen LJ, Shi J, Morita H, Nishida M, Honda A, Ito H. Transient receptor potential channels in cardiovascular function and disease. *Circ Res*. 2006; 99:119–131. [PubMed: 16857972]
8. Clapham DE. TRP channels as cellular sensors. *Nature*. 2003; 426:517–524. [PubMed: 14654832]
9. Shiroshita-Takeshita A, Brundel BJ, Burstein B, Leung TK, Mitamura H, Ogawa S, Nattel S. Effects of simvastatin on the development of the atrial fibrillation substrate in dogs with congestive heart failure. *Cardiovasc Res*. 2007; 74:75–84. [PubMed: 17270161]
10. Blaauw Y, Gögelein H, Tieleman RG, van Hunnik A, Schotten U, Allessie MA. “Early” class III drugs for the treatment of atrial fibrillation: efficacy and atrial selectivity of AVE0118 in remodeled atria of the goat. *Circulation*. 2004; 110:1717–1724. [PubMed: 15364815]
11. Li D, Fareh S, Leung TK, Nattel S. Promotion of atrial fibrillation by heart failure in dogs: atrial remodeling of a different sort. *Circulation*. 1999; 100:87–95. [PubMed: 10393686]
12. Sakabe M, Shiroshita-Takeshita A, Maguy A, Dumesnil C, Nigam A, Leung TK, Nattel S. Omega-3 polyunsaturated fatty acids prevent atrial fibrillation associated with heart failure but not atrial tachycardia remodeling. *Circulation*. 2007; 116:2101–2109. [PubMed: 17967774]
13. Gaborit N, Le Bouter S, Szuts V, Varro A, Escande D, Nattel S, Demolombe S. Regional and tissue specific transcript signatures of ion channel genes in the non-diseased human heart. *J Physiol*. 2007; 582:675–693. [PubMed: 17478540]

14. Mestdagh P, Van Vlierberghe P, De Weer A, Muth D, Westermann F, Speleman F, Vandesompele J. A novel and universal method for microRNA RT-qPCR data normalization. *Genome Biol.* 2009; 10:R64. [PubMed: 19531210]
15. Rose RA, Hatano N, Ohya S, Imaizumi Y, Giles WR. C-type natriuretic peptide activates a non-selective cation current in acutely isolated rat cardiac fibroblasts via natriuretic peptide C receptor-mediated signalling. *J Physiol.* 2007; 580:255–274. [PubMed: 17204501]
16. Burstein B, Libby E, Calderone A, Nattel S. Differential behaviors of atrial versus ventricular fibroblasts: a potential role for platelet-derived growth factor in atrial-ventricular remodeling differences. *Circulation.* 2008; 117:1630–1641. [PubMed: 18347210]
17. Ledoux J, Taylor MS, Bonev AD, Hannah RM, Solodushko V, Shui B, Tallini Y, Kotlikoff MI, Nelson MT. Functional architecture of inositol 1,4,5-triphosphate signaling in restricted spaces of myoendothelial projections. *Proc Natl Acad Sci U S A.* 2008; 105:9627–9632. [PubMed: 18621682]
18. Xiao J, Lin H, Luo X, Luo X, Wang Z. miR-605 joins p53 network to form a p53:miR-605:Mdm2 positive feedback loop in response to stress. *EMBO J.* 2011; 30:524–532. [PubMed: 21217645]
19. Kiyonaka S, Kato K, Nishida M, Mio K, Numaga T, Sawaguchi Y, Yoshida T, Wakamori M, Mori E, Numata T, Ishii M, Takemoto H, Ojida A, Watanabe K, Uemura A, Kurose H, Morii T, Kobayashi T, Sato Y, Sato C, Hamachi I, Mori Y. Selective and direct inhibition of TRPC3 channels underlies biological activities of a pyrazole compound. *Proc Natl Acad Sci U S A.* 2009; 106:5400–5405. [PubMed: 19289841]
20. Hofmann T, Obukhov AG, Schaefer M, Harteneck C, Gudermann T, Schultz G. Direct activation of human TRPC6 and TRPC3 channels by diacylglycerol. *Nature.* 1999; 397:259–263. [PubMed: 9930701]
21. Pagès G, Lenormand P, L'Allemain G, Chambard JC, Meloche S, Pouyssegur J. Mitogen-activated protein kinases p42mapk and p44mapk are required for fibroblast proliferation. *Proc Natl Acad Sci U S A.* 1993; 90:8319–8323. [PubMed: 8397401]
22. Dudley DT, Pang L, Decker SJ, Bridges AJ, Saltiel AR. A synthetic inhibitor of the mitogen-activated protein kinase cascade. *Proc Natl Acad Sci U S A.* 1995; 92:7686–7689. [PubMed: 7644477]
23. Dietrich A, Mederos y Schnitzler M, Kalwa H, Storch U, Gudermann T. Functional characterization and physiological relevance of the TRPC3/6/7 subfamily of cation channels. *Naunyn Schmiedebergs Arch Pharmacol.* 2005; 371:257–265. [PubMed: 15909153]
24. Jia Y, Zhou J, Tai Y, Wang Y. TRPC channels promote cerebellar granule neuron survival. *Nat Neurosci.* 2007; 10:559–567. [PubMed: 17396124]
25. Reading SA, Earley S, Waldron BJ, Welsh DG, Brayden JE. TRPC3 mediates pyrimidine receptor-induced depolarization of cerebral arteries. *Am J Physiol Heart Circ Physiol.* 2005; 288:H2055–H2061. [PubMed: 15604128]
26. Philipp S, Strauss B, Hirnet D, Wissenbach U, Mery L, Flockerzi V, Hoth M. TRPC3 mediates T-cell receptor-dependent calcium entry in human T-lymphocytes. *J Biol Chem.* 2003; 278:26629–26638. [PubMed: 12736256]
27. Onohara N, Nishida M, Inoue R, Kobayashi H, Sumimoto H, Sato Y, Mori Y, Nagao T, Kurose H. TRPC3 and TRPC6 are essential for angiotensin II-induced cardiac hypertrophy. *EMBO J.* 2006; 25:5305–5316. [PubMed: 17082763]
28. Wu X, Eder P, Chang B, Molkentin JD. TRPC channels are necessary mediators of pathologic cardiac hypertrophy. *Proc Natl Acad Sci U S A.* 2010; 107:7000–7005. [PubMed: 20351294]
29. Nishida M, Onohara N, Sato Y, Suda R, Ogushi M, Tanabe S, Inoue R, Mori Y, Kurose H. Gα12/13-mediated up-regulation of TRPC6 negatively regulates endothelin-1-induced cardiac myofibroblast formation and collagen synthesis through nuclear factor of activated T cells activation. *J Biol Chem.* 2007; 282:23117–23128. [PubMed: 17533154]
30. Du J, Xie J, Zhang Z, Tsujikawa H, Fusco D, Silverman D, Liang B, Yue L. TRPM7-mediated Ca²⁺ signals confer fibrogenesis in human atrial fibrillation. *Circ Res.* 2010; 106:992–1003. [PubMed: 20075334]

31. Mio K, Ogura T, Kiyonaka S, Hiroaki Y, Tanimura Y, Fujiyoshi Y, Mori Y, Sato C. The TRPC3 channel has a large internal chamber surrounded by signal sensing antennas. *J Mol Biol.* 2007; 367:373–383. [PubMed: 17258231]
32. Numaga T, Nishida M, Kiyonaka S, Kato K, Katano M, Mori E, Kurotaki T, Inoue R, Hikida M, Putney JW Jr, Mori Y. Ca^{2+} influx and protein scaffolding via TRPC3 sustain $\text{PKC}\beta$ and ERK activation in B cells. *J Cell Sci.* 2010; 123:927–938. [PubMed: 20179100]
33. Olson ER, Shamhart PE, Naugle JE, Meszaros JG. Angiotensin II-induced extracellular signal-regulated kinase 1/2 activation is mediated by protein kinase C δ and intracellular calcium in adult rat cardiac fibroblasts. *Hypertension.* 2008; 51:704–711. [PubMed: 18195168]
34. Qi XY, Yeh YH, Xiao L, Burstein B, Maguy A, Chartier D, Villeneuve LR, Brundel BJJM, Dobrev D, Nattel S. Cellular signalling underlying atrial tachycardia remodeling of L-type calcium-current. *Circ Res.* 2008; 103:845–854. [PubMed: 18723446]
35. Kozak JA, Cahalan MD. MIC channels are inhibited by internal divalent cations but not ATP. *Biophys J.* 2003; 84:922–927. [PubMed: 12547774]
36. Nadler MJ, Hermosura MC, Inabe K, Perraud AL, Zhu Q, Stokes AJ, Kurotaki T, Kinet JP, Penner R, Scharenberg AM, Fleig A. LTRPC7 is a Mg.ATP-regulated divalent cation channel required for cell viability. *Nature.* 2001; 411:590–595. [PubMed: 11385574]
37. Avitall B, Bi J, Myktysey A, Chicos A. Atrial and ventricular fibrosis induced by atrial fibrillation: evidence to support early rhythm control. *Heart Rhythm.* 2008; 5:839–845. [PubMed: 18534368]

CLINICAL PERSPECTIVE

Atrial fibrillation (AF) is the most common clinical arrhythmia, and its therapy is problematic. There is a need for novel treatment interventions, and mechanistic insights may be helpful in developing such new therapies. Here, we examined the role of a new type of ion channel, the nonselective cation channel TRPC3 (transient receptor potential canonical-3), in AF. TRPC3 can carry a number of ions but may be particularly important as an entry pathway for calcium into nonexcitable cells such as fibroblasts. Tissue fibrosis is produced by an overproduction of extracellular matrix proteins by fibroblasts and is believed to be important in AF. In addition, fibroblasts may contribute to AF via electric interactions with excitable heart cells (cardiomyocytes). We first found that cardiac fibroblasts expressed functional TRPC3 channels, and TRPC3-mediated calcium entry into fibroblasts activated a signaling molecule (extracellular signal-regulated kinase) that induced fibroblast proliferation and differentiation into activated myofibroblasts. We also noted that TRPC3 expression was upregulated in AF patients and 2 experimental AF models. We then studied the role of TRPC3 in atrial remodeling of dogs kept in AF for 7 days by atrial tachypacing. We found that AF increased TRPC3 protein expression and current, although it activated fibroblasts, and that blocking TRPC3 suppressed fibroblast activation and the AF-promoting remodeling caused by AF. We also identified the molecular pathway that leads to TRPC3 upregulation in AF: Downregulation of a TRPC3-suppressing microRNA, miR-26, caused by AF-induced nuclear translocation/regulation by nuclear factor of activated T-lymphocytes (NFAT) in fibroblasts. This work provides novel insights into molecular mechanisms underlying AF, as well as potential new anti-AF targets.

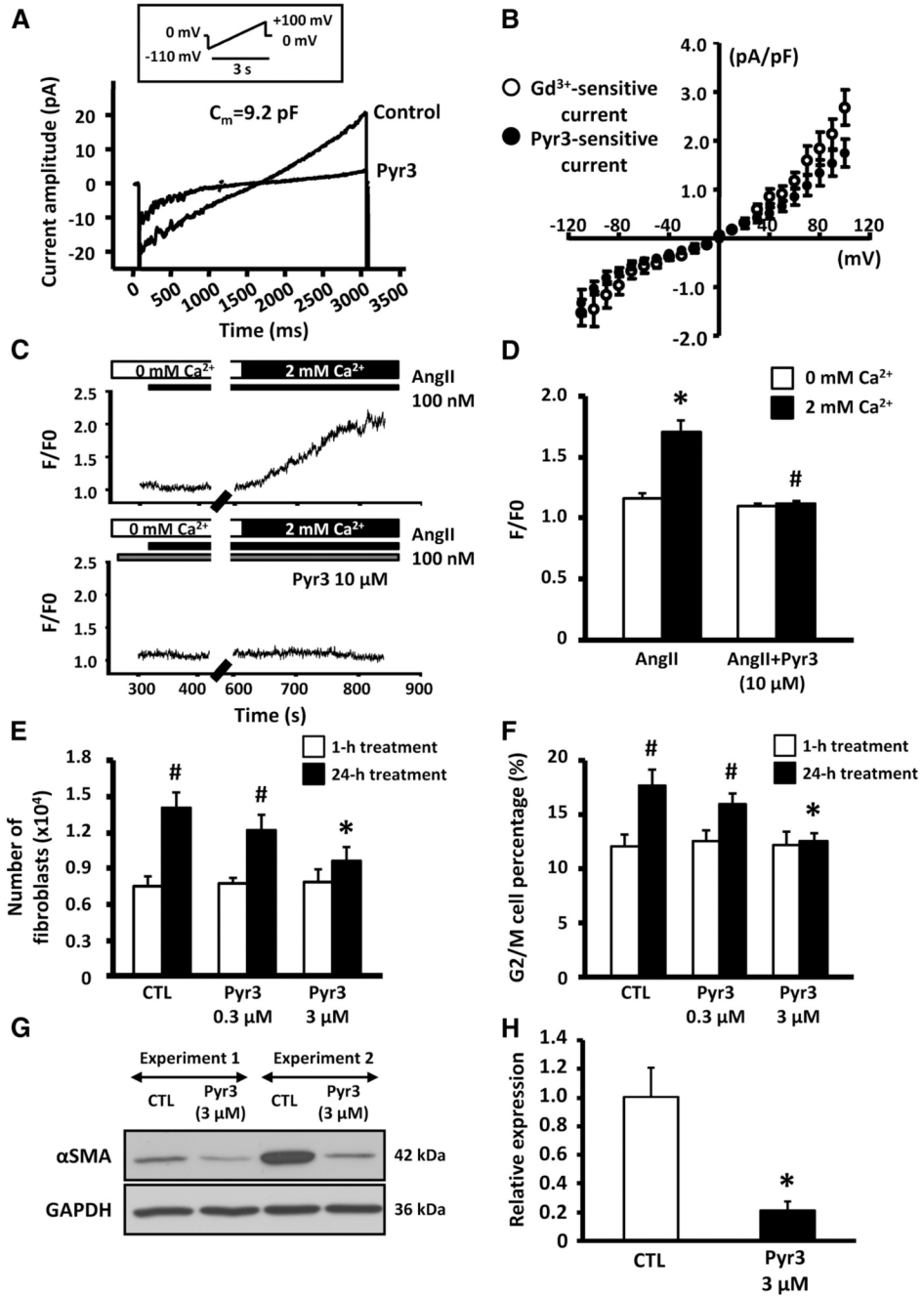


Figure 1.

A, Representative nonselective cation current (I_{NSC}) recordings with or without pyrazole-3 (Pyr3; 3 μ mol/L). **B**, Mean \pm SEM Gd^{3+} - and Pyr3-sensitive I_{NSC} density (n=7 cells in Gd^{3+} and 9 cells in Pyr3). **C**, Recordings of angiotensin II (AngII)-induced intracellular Ca^{2+} response in presence or absence of Pyr3. **D**, Mean \pm SEM AngII-induced Ca^{2+} fluorescence (F/F₀), normalized to baseline in 0 mmol/L Ca^{2+} (n=18 and 20 cells in AngII and AngII with Pyr3, respectively; * P <0.05 vs 0 mmol/L Ca^{2+} , # P <0.05 vs 2 mmol/L Ca^{2+} in AngII). **E**, Mean \pm SEM fibroblast count after 1- or 24-hour culture with vehicle control (CTL) or 0.3 or 3 μ mol/L Pyr3 (n=9/group; * P <0.05 vs CTL, # P <0.05 vs 1-hour treatment). **F**, Mean \pm SEM

percentage of cells in G₂/M phase after Pyr3 treatment (n=9; **P*<0.05 vs CTL, #*P*<0.05 vs 1-hour treatment). **G**, Representative immunoblots for α -smooth muscle actin (α SMA) and GAPDH in rat fibroblasts cultured with or without Pyr3 (3 μ mol/L). **H**, Mean \pm SEM α SMA/GAPDH expression ratio (n=8/group; **P*<0.05 vs CTL).

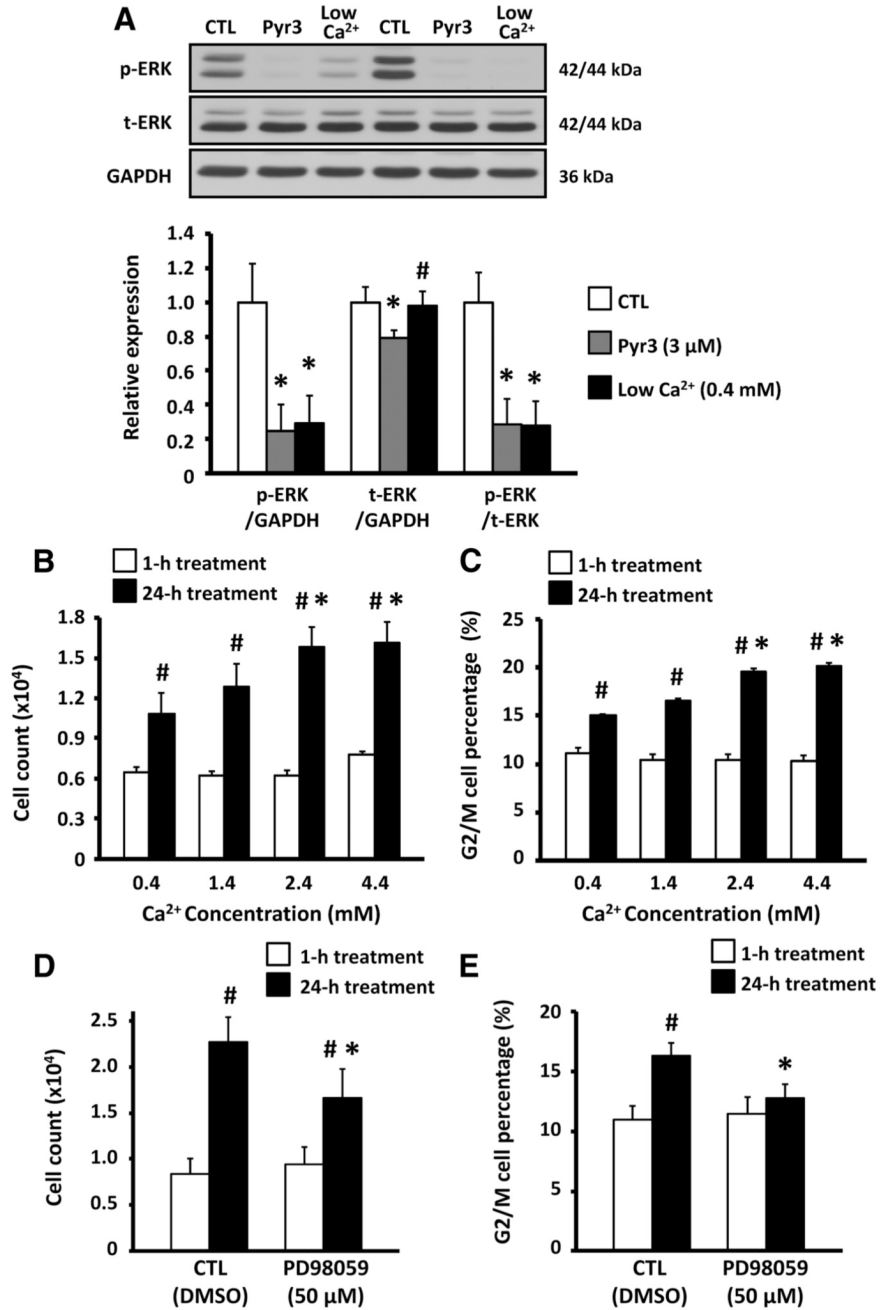


Figure 2.

A, Top, Representative immunoblots of phosphorylated extracellular signal-regulated kinase (ERK)-1/2 (p-ERK), total ERK-1/2 (t-ERK), and GAPDH in rat fibroblasts cultured with 0.4 mmol/L Ca²⁺, 2.4 mmol/L Ca²⁺, and 2.4 mmol/L Ca²⁺ medium containing 3 μmol/L pyrazole-3 (Pyr3). CTL indicates control. **Bottom**, Mean±SEM p-ERK/GAPDH, t-ERK/GAPDH, and p-ERK/t-ERK (n=8/group; *P<0.05 vs CTL, #P<0.05 vs Pyr3). **B**, Mean±SEM fibroblast cell count after culture in M199 medium containing 0.4 to 4.4 mmol/L Ca²⁺ (n=8/group; *P<0.05 vs 0.4-mmol/L Ca²⁺, #P<0.05 vs 1-hour treatment). **C**, Mean±SEM percentage of cells in G₂/M phase (n=8/group; *P<0.05 vs 0.4-mmol/L Ca²⁺, #P<0.05 vs 1-hour treatment). **D**, Mean±SEM fibroblast cell count after 1- and 24-hour

treatment with 50 $\mu\text{mol/L}$ PD98059 (n=6/group; * $P<0.05$ vs CTL, # $P<0.05$ vs 1-hour treatment). E, Mean \pm SEM percentage of cells in G₂/M phase after 50 $\mu\text{mol/L}$ PD98059 treatment (n=6/ group; * $P<0.05$ vs CTL).

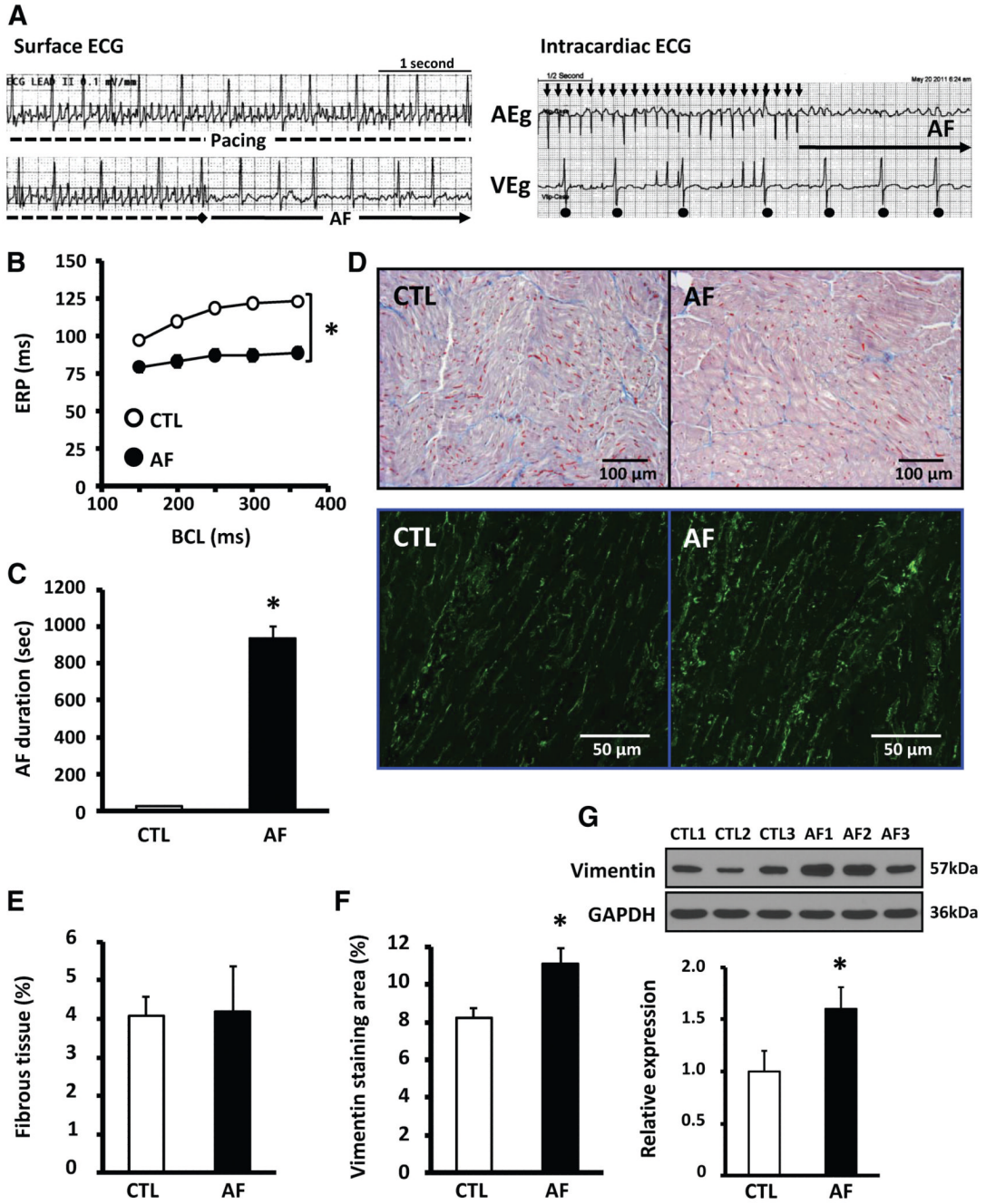


Figure 3.

A, Representative surface ECG (**left**) and intracardiac electrograms (**right**) in an awake dog with atrial fibrillation (AF) on day 7. **B**, Mean \pm SEM atrial effective refractory period (ERP) in control (CTL; n=11) and AF dogs (n=12) on day 7 (* P <0.05). BCL indicates basic cycle length. **C**, Mean \pm SEM duration of induced AF (* P <0.05 vs CTL). **D**, **Top**, Representative Masson's trichrome-stained left atrial images from CTL (left) and AF (right) dogs. **Bottom**, Representative immunofluorescent images of LA free-wall tissues stained with vimentin. **E**, Mean \pm SEM fibrous tissue content in left atrial free-wall tissues (n=5 CTL, 5 AF dogs). **F**, Mean \pm SEM vimentin-positive area (n=5 CTL, 5 AF dogs; * P <0.05 vs CTL). **H**,

Representative immunoblots (**top**) and mean \pm SEM vimentin band intensity normalized to GAPDH (**bottom**) in left atrial samples from CTL (n=5) and AF dogs (n=5; * P <0.05 vs CTL).

Results in Freshly-Isolated Fibroblasts

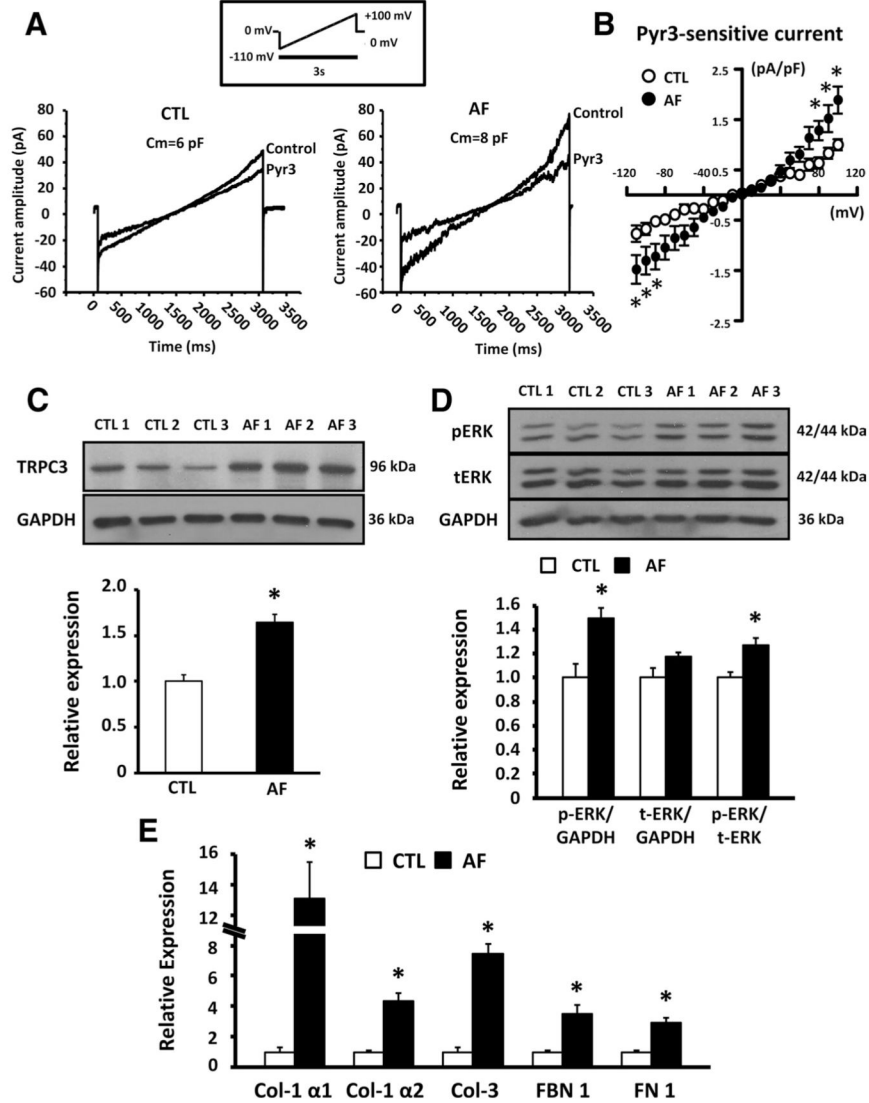


Figure 4.

A, Representative nonselective cation current (I_{NSC}) recordings before and after pyrazole-3 (Pyr3; 3 μ mol/L) in freshly isolated left atrial fibroblasts from control (CTL) dogs and dogs with tachypacing-induced atrial fibrillation (AF). **B**, Mean \pm SEM Pyr3-sensitive I_{NSC} density in CTL dogs (n=6 dogs, 8 cells) and AF dogs (n=6 dogs, 9 cells; $P<0.05$ vs CTL). **C**, Representative immunoblots (**top**) and mean \pm SEM TRPC3 subunit band intensity relative to GAPDH (**bottom**) in freshly isolated left atrial fibroblasts from CTL (n=6) and AF dogs (n=6; $*P<0.05$ vs CTL). **D**, Representative immunoblots (**top**) and mean \pm SEM data (**bottom**) for phosphorylated (p-ERK-1/2) and total (t-ERK-1/2) extracellular signal-regulated kinase 1/2 (ERK-1/2) relative to GAPDH. **E**, Mean \pm SEM extracellular matrix gene mRNA expression in freshly isolated left atrial fibroblasts (n=6 CTL and 6 AF; $*P<0.05$ vs CTL). Col indicates collagen; FBN, fibrinogen; FN, fibronectin.

Results in Cultured Fibroblasts

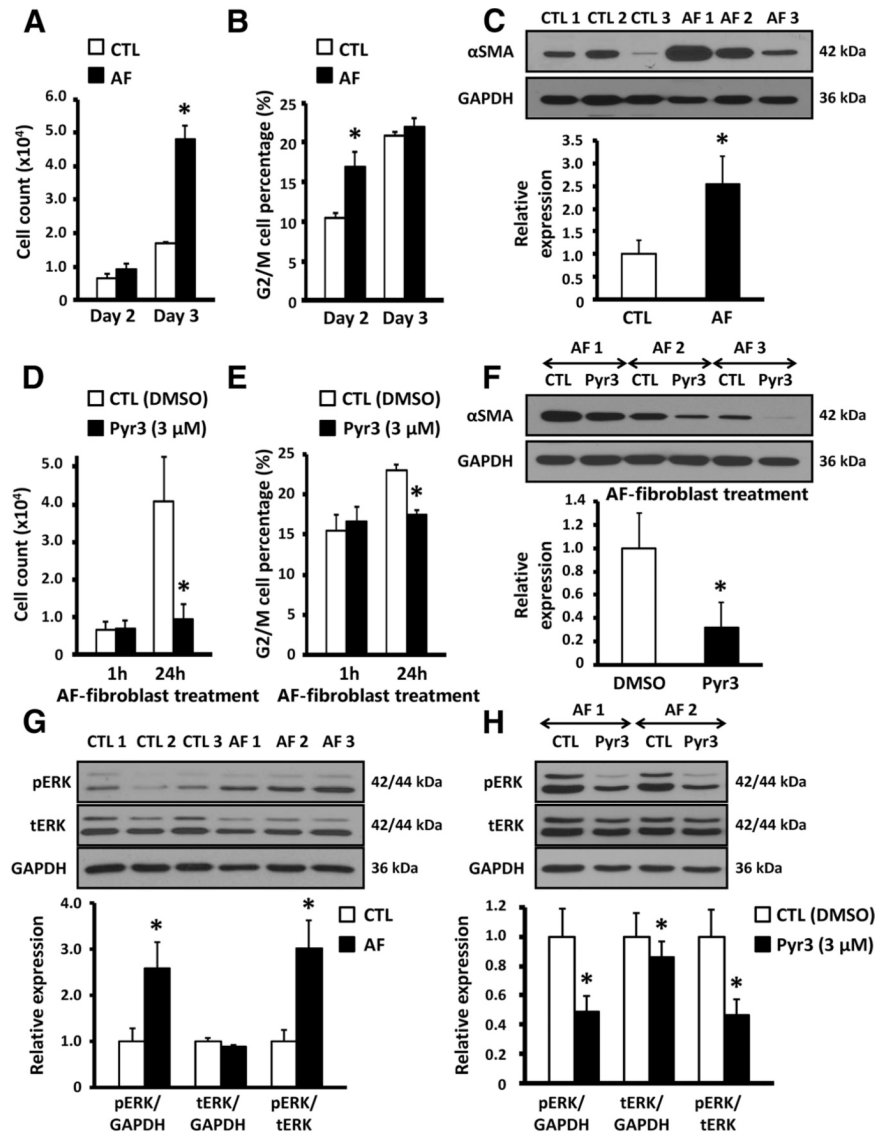


Figure 5. **A**, Mean±SEM cell count of left atrial fibroblasts after 2- and 3-day culture in control dogs (CTL; n=7) and dogs with tachypacing-induced atrial fibrillation (AF; n=7; **P*<0.05 vs CTL). **B**, Mean±SEM percentage of cells in G₂/M phase (n=7 dogs/group; **P*<0.05 vs CTL). **C**, Representative immunoblots (**top**) and mean±SEM α -smooth muscle actin/GAPDH (α SMA; **bottom**) in cultured left atrial fibroblasts from CTL (n=6) and AF dogs (n=7; **P*<0.05 vs CTL). **D**, Mean±SEM cell count of left atrial fibroblasts after 1- or 24-hour culture with vehicle/control or pyrazole-3 (Pyr3; 3 μ mol/L) in AF dogs (n=6/group; **P*<0.05 vs DMSO). **E**, Mean±SEM percentage of cells in G₂/M phase (n=6/group; **P*<0.05 vs DMSO). **F**, Representative immunoblots (**top**) and mean±SEM α -SMA/GAPDH expression ratios (**bottom**) in cultured left atrial fibroblasts from AF dogs (n=7) in the presence of vehicle (DMSO) or Pyr3 (**P*<0.05 vs DMSO). **G**, Representative immunoblots (**top**) and mean±SEM phosphorylated extracellular signal-regulated kinase-1/2 (pERK) and total ERK-1/2 (tERK) relative to GAPDH (**bottom**) in cultured left atrial fibroblasts of CTL

and AF dogs (n=6/group; * P <0.05 vs CTL). **H**, Representative immunoblots (**top**) and mean \pm SEM ERK (bottom) in left atrial fibroblasts from AF dogs cultured with vehicle (DMSO) or Pyr3 (3 μ mol/L, n=6/group; * P <0.05 vs DMSO).

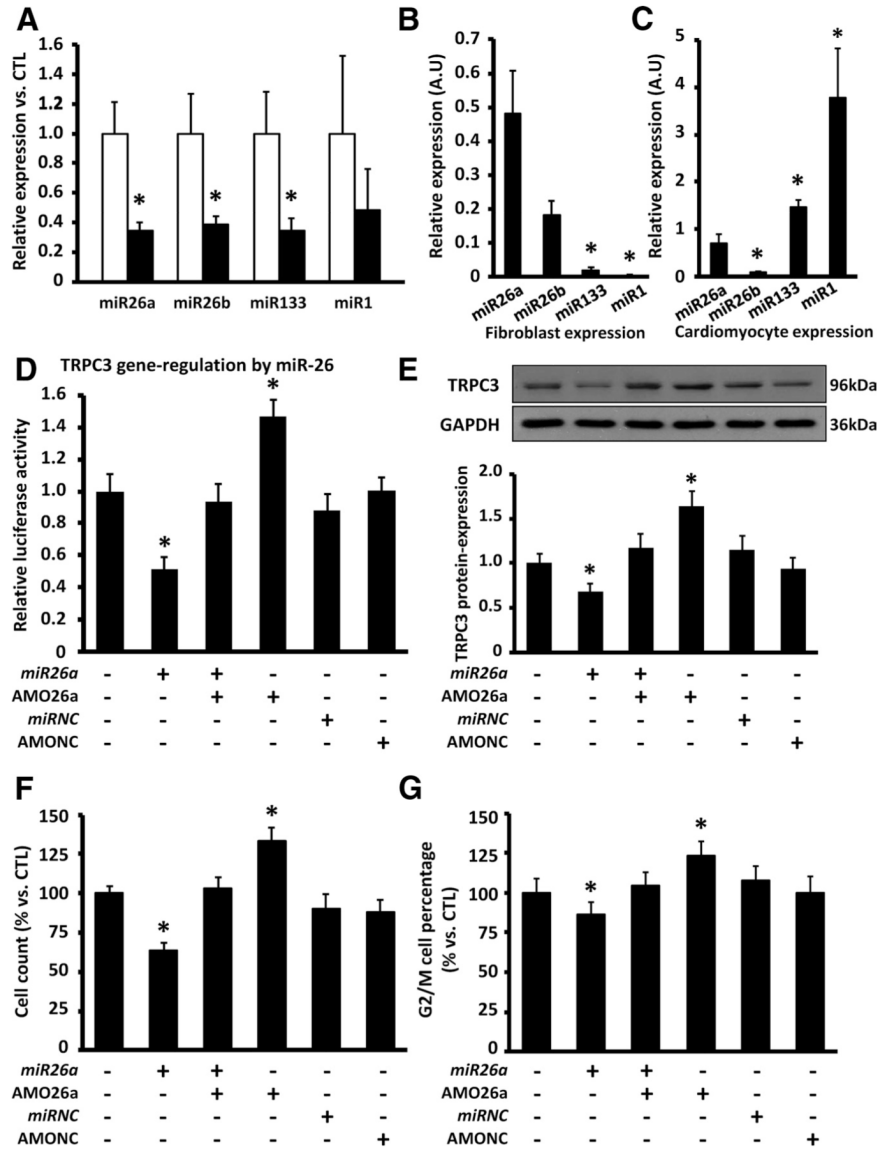


Figure 6. **A**, Mean±SEM microRNA expression in freshly isolated left atrial fibroblasts in dogs with tachypacing-induced atrial fibrillation (AF; n=7) and control dogs (CTL; n=7; *P<0.05 vs CTL). **B**, Mean±SEM relative microRNA expression in freshly isolated left atrial fibroblasts in CTL (n=5; *P<0.05 vs miR-26a). A.U. indicates arbitrary units. **C**, Mean±SEM relative microRNA expression in freshly isolated left atrial cardiomyocytes in CTL (n=5; *P<0.05 vs miR-26a). **D**, Mean±SEM relative luciferase activity in HEK293 cells transfected with miR-26a overexpression (miR-26a duplex) or knockdown (anti-sense anti-miR-26a oligonucleotides [AMO26a]) probes (n=7/group; P<0.05 vs cells transfected without the miR-26a probes). **E**, Representative immunoblots (**top**) and mean±SEM TRPC3/GAPDH protein expression (**bottom**) in dog left atrial fibroblasts transfected with the miR-26a duplex or AMO26a (n=7; P<0.05 vs cells without miR-26a probes). **F**, Mean±SEM fibroblast count in dog left atrial fibroblasts transfected with miR-26a duplex or AMO26a (n=7/ group; *P<0.05 vs cells transfected without miR-26a probes). **G**, Mean±SEM

percentage of cells in G₂/M phase (n=7/group; **P*<0.05 vs cells transfected without miR-26a probes).

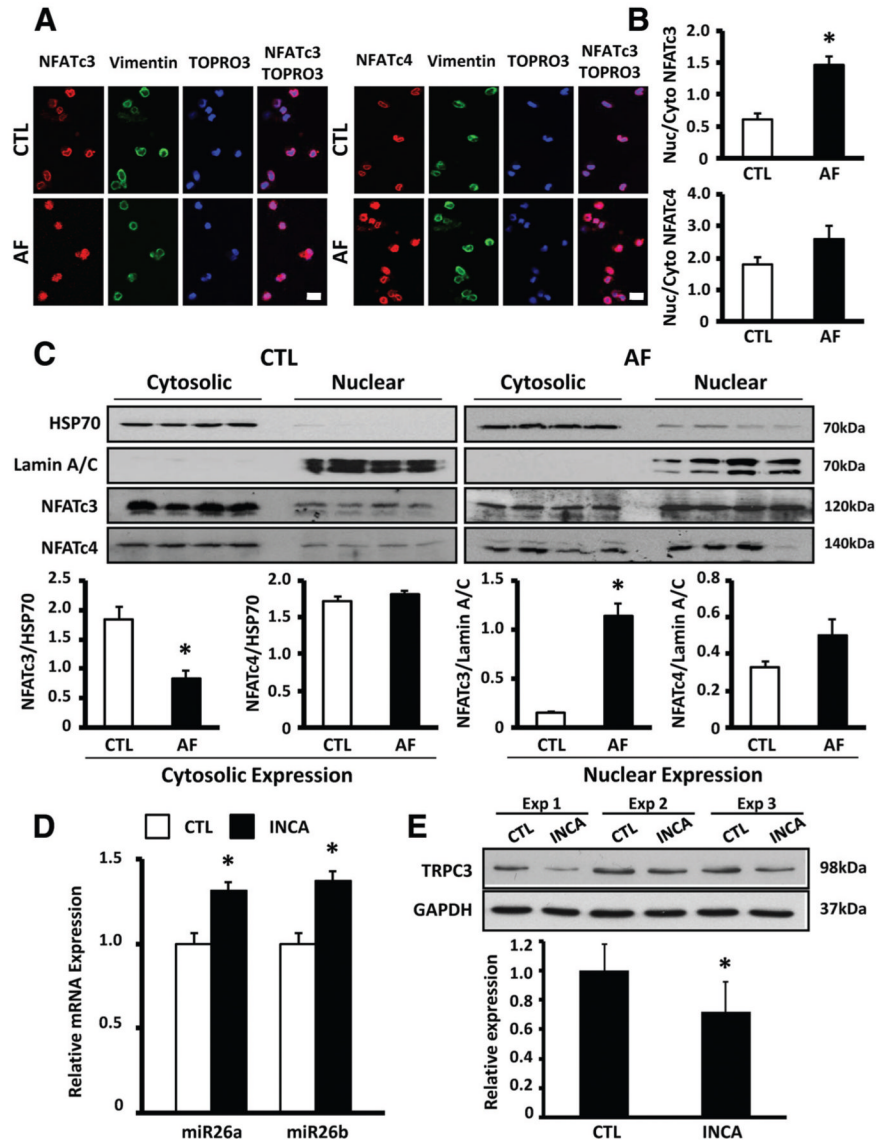
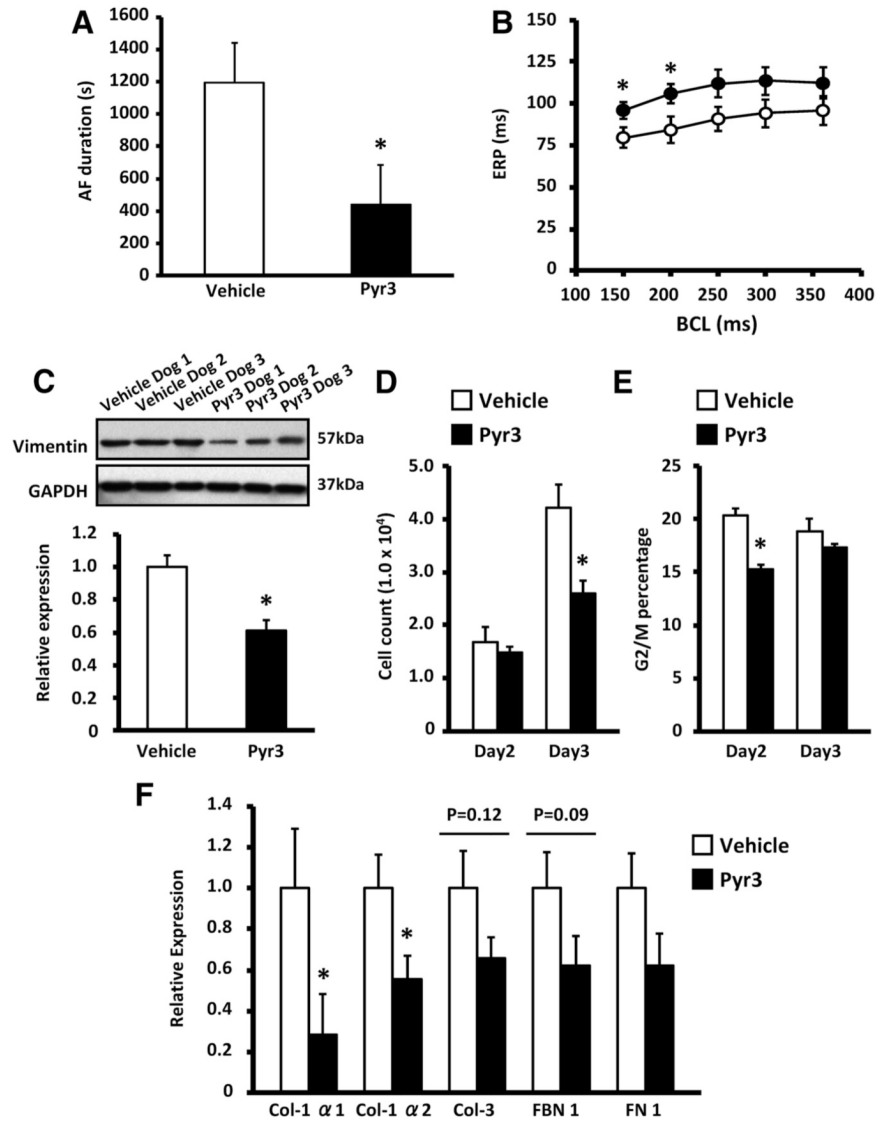


Figure 7.

A, Representative immunofluorescent images of freshly isolated left atrial fibroblasts stained with NFATc3/ NFATc4, vimentin (fibroblast marker), and TOPRO-3 (nuclear marker) antibodies in dogs with tachypacing-induced atrial fibrillation (AF) and control dogs (CTL). **B**, Mean±SEM nuclear/cytoplasmic (Nuc/Cyto) signal intensity ratio of NFATc3 (**top**) and NFATc4 (**bottom**; n=5; *P<0.05 vs CTL). **C**, **Top**, Representative immunoblots of cytosolic and nuclear protein fractions of HSP70 (cytosolic marker), lamin A/C (nuclear marker), NFATc3, and NFATc4 in freshly isolated left atrial fibroblasts in AF and CTL dogs. **Bottom**, Mean±SEM cytoplasmic NFATc3/NFATc4 relative to HSP70 and nuclear NFATc3/NFATc4 relative to lamin A/C (n=4/group; *P<0.05 vs CTL). **D**, Mean±SEM miR-26a and miR-26b expression in control dog left atrial fibroblasts treated with INCA6 (2.5 μmol/L) for 24 hours (n=5/ group; *P<0.05 vs DMSO). **E**, Representative immunoblots (**top**) and mean±SEM TRPC3/GAPDH (**bottom**) in control dog left atrial fibroblasts treated with INCA6 (2.5 μmol/L) for 24 hours (n=5; *P<0.05 vs DMSO).

**Figure 8.**

A, Mean \pm SEM duration of induced atrial fibrillation (AF) on day 7 in AF dogs treated throughout the AF pacing period with intravenous pyrazole-3 (Pyr3; n=6, 0.1 mg \cdot kg⁻¹ \cdot d⁻¹) or vehicle (n=6, **P*<0.05 vs vehicle). **B**, Mean \pm SEM atrial effective refractory period (ERP; open circles indicate vehicle; filled circles, Pyr3; **P*<0.05 vs vehicle). BCL indicates basic cycle length. **C**, Representative immunoblots (**top**) and mean \pm SEM vimentin band intensity normalized to GAPDH (**bottom**) in left atrial tissue samples from Pyr3-treated (n=5) or vehicle-treated AF dogs (n=5; **P*<0.05 vs vehicle). **D**, Mean \pm SEM cell count of left atrial fibroblasts after 2- and 3-day culture in Pyr3-treated (n=6) or vehicle-treated AF dogs (n=6; **P*<0.05 vs vehicle). **E**, Mean \pm SEM percentage of cells in G₂/M phase (n=6/group; **P*<0.05 vs vehicle). **F**, Mean \pm SEM extracellular matrix gene mRNA expression in freshly isolated left atrial fibroblasts from Pyr3-treated (n=5) or vehicle-treated AF dogs (n=5; **P*<0.05 vs vehicle). Col indicates collagen; FBN, fibrinogen; FN, fibronectin.